Physica B 186–188 (1993) 212–217
North-Holland

PHYSICA B

On the magnetic and superconducting phases of heavy-fermion UPt_3

A. de Visser, N.H. van Dijk, K. Bakker and J.J.M. Franse
Van der Waals–Zeeman Laboratorium, Universiteit van Amsterdam, The Netherlands

The electronic instability in the highly correlated electron system UPt_3 gives rise to various intriguing phenomena at liquid-helium temperatures, among which the occurrence of unconventional superconductivity ($T_c^+ = 0.49$ K, $T_c^- = 0.44$ K) has attracted most attention. In a magnetic field three superconducting phases are observed that meet at a tetracritical point. We here present a discussion of a number of puzzling aspects of a superconducting phase diagram ($B \perp c$) of unprecedented accuracy, determined by dilatometry. The possible interplay of superconductivity and reduced moment antiferromagnetism ($T_N = 5$ K) is investigated. Furthermore, we report on recent studies of the suppression of T_c, by alloying with Pd, Y, Th, Au and Ir.

1. Introduction

Among the U-based intermetallics, UPt_3 has attracted by far the most attention because of its unrivalled low-temperature properties [1]. Below ~20 K, competing electron–electron interactions give rise to the formation of a narrow quasiparticle band close to the Fermi level and the concurrent strongly renormalized electron properties. In addition, antiferromagnetic order ($T_N = 5$ K), with extremely small ordered moments ($0.02\mu_B$/U-atom), and unconventional superconductivity ($T_c^+ = 0.49$ K and $T_c^- = 0.44$ K) are found. Most of these intriguing properties have been studied on high-quality single-crystalline samples allowing for detailed experimental investigations.

Immediately after the discovery of superconductivity in heavy-fermion UPt_3 it was recognized that its superconducting properties are unconventional. The occurrence of a superconducting instability in the heavy-electron liquid gave rise to speculations about an unconventional electron–electron pairing mechanism and an unusual symmetry of the Cooper pairs. As to the symmetry of the pairing function, measurements of the sound attenuation [2] and the London penetration depth [3] revealed a power-law behaviour in the temperature dependence of the electronic excitations over the gap and a strongly anisotropic response, indicating a hybrid gap with line nodes at the equator and point nodes at the poles. However, as impurity scattering may contribute significantly, the determination of the gap function is not unambiguous.

During the last two years research has been directed towards more solid evidence for unconventional superconductivity in UPt_3, namely the observation of additional anomalies in the thermodynamic quantities of the superconducting phase. Measurements of the specific heat [4], sound velocity [5,6] and thermal expansion [7] on high-quality single-crystalline samples, clearly identified a second phase transition that takes place ~50 mK below T_c^+. Moreover, measurements in an external magnetic field revealed a complex superconducting phase diagram with three distinctly different phases that meet at a tetracritical point [5–8]. From the theoretical side much effort has been put in a phenomenological interpretation of the phase diagram within the Ginzburg–Landau (GL) formalism including a coupling term which describes the interaction of the superconducting order parameter (OP) with a symmetry-breaking field (SBF) [9]. Although this analysis yields a superconducting vector OP, it does not enable the distinction between a d- or p-wave state. In the most appealing scenario the SBF originates from the extremely small antiferromagnetic (AF) moment ($0.02\mu_B$/U-atom) detected by neutron diffraction below $T_N = 5$ K [10]. This scenario has triggered several experimental studies that aimed to probe a coupling of the AF and superconducting OP. On the other hand, the available GL models are inadequate at several points [11], which urges for further theoretical and experimental investigations. In

Correspondence to: A. de Visser, Van der Waals–Zeeman Laboratorium, Universiteit van Amsterdam, Valckenierstraat 65, 1018 XE Amsterdam, The Netherlands.

the following we report on recent experimental work concerning the puzzling aspects of the magnetic and superconducting phases of UPt_3.

2. The superconducting phase diagram

The study of the double superconducting transition of UPt_3 ($T_c^+ = 0.49$ K, $T_c^- = 0.44$ K) in a magnetic field has led to the discovery of a remarkable phase diagram in the B–T plane with four phase lines that meet at a tetracritical point. The first diagrams were constructed from the results collected by means of different experimental techniques (electrical resistivity, specific heat, thermal expansion, sound attenuation and thermal conductivity) [7,8] and therefore lacked a high accuracy. Later, Bruls et al. [5] and Adenwalla et al. [6] identified all four phase lines with one single technique, namely sound velocity measurements. Furthermore, they showed that the topology of the phase diagram for B along and perpendicular to the hexagonal (c-)axis is essentially the same, although the location of the tetracritical point differs.

Recently, van Dijk et al. [12] performed an accurate dilatometry study of the superconducting phases. The thermal expansion (α_c) and magnetostriction (λ_c) were measured for an elongation (contraction) along the c-axis and a field applied along either the a- or b-axis in the hexagonal plane. Several anomalies were detected and identified with the normal to superconducting phase transition, or phase transitions within the superconducting state. The resulting phase diagram is of unprecedented accuracy. It is shown in fig. 1, where the three superconducting phases are labeled A, B and C. No anisotropy for fields in the basal plane was observed. A close inspection of the region near the critical point (see fig. 2) clearly reveals that the phase diagram has a *tetra*critical point located at $T_{cr} = 0.387(3)$ K and $B_{cr} = 0.443(5)$ T. The thermodynamic stability of the phase diagram has been investigated by Yip et al. [13]. The $c(T)$ measurements indicate that the NA, AB and NC phase lines are of second order, since no latent heat is observed. The BC phase line has not been probed by the specific heat so far, but its order can be inferred from the thermodynamic constraints on the phase diagram, that relate the slopes of the phase lines near the tetracritical point to the discontinuities in the specific heat at the phase transitions. For the phase diagram in fig. 1 the relevant slopes near the tetracritical point (solid lines in fig. 2) equal $dT_{NA}/dB = -0.241$ K/T, $dT_{AB}/dB = -0.070$ K/T, $dT_{BC}/dB = -0.840$ K/T and $dT_{NC}/dB = -0.188$ K/T, while the specific heat data published in ref. [8] yield jump ratios $\Delta C_{NA}/\Delta C_{NC} = 0.65$ and $\Delta C_{AB}/\Delta C_{NC} = 0.35$. With these parameters we conclude that the BC transition is also of second order, which is supported by the absence of hysteresis in the magnetostriction at the BC transition. Recently, Adenwalla et al. [14] concluded that the phase diagram can only be stable if the BC phase line is of first order. However their analysis of the specific heat jumps yields $\Delta C_{NA}/\Delta C_{NC} = 1$ and $\Delta C_{AB}/\Delta C_{NC} = 0$, which is inconsistent with experiments. Accurate measurements of the step size in the specific heat near the tetracritical point may further elucidate this point.

The pressure dependence of the superconducting phase diagram can be determined via the Ehrenfest relations for second-order phase transitions. So far, only the thermal expansion and magnetostriction

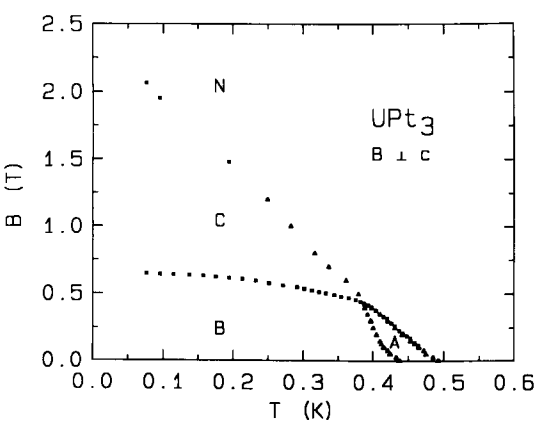

Fig. 1. Superconducting phase diagram of UPt_3 for $B \perp c$, determined from magnetostriction (■) and thermal-expansion (▲) data (after ref. [12]).

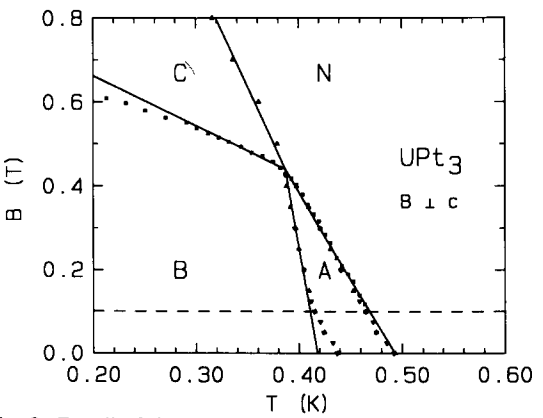

Fig. 2. Detail of the superconducting phase diagram of UPt_3 near the tetracritical point. The phase lines are obtained from thermal-expansion data for $B \| b$ (▲) and $B \| a$ (▼) and from magnetostriction data for $B \| b$ (■). The full lines represent the slopes near (T_{cr}, B_{cr}). The dashed line locates the temperature-independent anomaly at $B_d = 0.1$ T [12].

along the c-axis have been measured [12], so that only the effect of a uniaxial pressure along c (p_c) can be evaluated. The pressure dependence of the NA, AB and NC phase lines can be calculated from the ratio of the discontinuities at the phase transitions observed in $\alpha_c(T)$ and $c(T)$. The pressure dependence of the remaining phase line (BC) can be calculated from the ratio of the discontinuities in the coefficient of magnetostriction (τ_c) and the elastic compliance s_{33} [5,6]. The resulting temperature–field–pressure phase diagram is schematically shown in fig. 3. This remarkable diagram shows that the C phase is the most stable phase under pressure. The A and B phases are suppressed rapidly and disappear at 2–3 kbar in zero field. The tetracritical point shifts to $T_{cr} = 0.46$ K and $p_{cr} = 2.5$ kbar in zero field, in accordance with the thermodynamic constraints [13] that dictate that also in the p_c–T plane a tetracritical point exists. In order to derive fig. 3, a linear pressure dependence of the phase lines was assumed. This approximation is justified by the good agreement with the zero-field p_c–T diagram deduced from recent $c(T)$ data under uniaxial pressure [15]. Note, however, that the $c(T)$ experiments did not probe the BC phase line. The absence of sizeable jumps at T_c^+ and T_c^- in the coefficient of thermal expansion for the basal plane (zero field) [7] indicates that the A and B phases are at least one order of magnitude less sensitive to stress in the plane than to stress along c.

The high-precision phase diagram revealed a novel feature near 0.1 T, namely, an abrupt change in the slope of the AB phase line. This anomalous behaviour concurs with a small anomaly detected at 0.1 T in $\lambda_c(B)$ for field directions in the basal plane (a- and b-axes). However, the anomaly is also observed in the magnetostriction of the normal phase [12] and therefore it cannot be attributed to superconductivity. We comment on this in section 4.

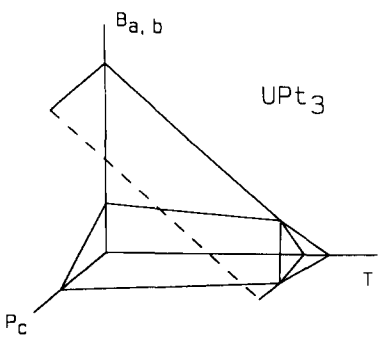

Fig. 3. The pressure dependence (stress along c) of the superconducting phases of UPt_3 for a field in the basal plane (after ref. [12]). The A and B phases disappear at moderate pressures (2–3 kbar in a zero field).

3. Ginzburg–Landau models

The zero-pressure phase diagram can be explained to a large extent by the Ginzburg–Landau formalism including a symmetry-breaking term. The E_{1g} representation model appears to be the most relevant model [9]. It is able to describe correctly the topology of the phase diagram for $B \perp c$. Furthermore, various quantities, such as the specific heat and the upper and lower critical field, can be analysed in a consistent way, yielding a ratio for the fourth-order stability parameters $\beta_2/\beta_1 \simeq 0.4$ [16]. Therefore, it is of interest to analyse the thermal-expansion and magnetostriction data in the same GL model. Here we follow the approach of Thalmeier et al. [17]. Symmetry arguments (UPt_3 has D_{6h} symmetry) lead to the choice of E_{1g} basis vectors for the OP. The hybrid gap function is given by $\psi(\boldsymbol{k}) = \eta_x k_x k_z + \eta_y k_y k_z$, where the complex vector $\boldsymbol{\eta} = (\eta_x, \eta_y) = (|\eta_x| e^{i\Phi_x}, |\eta_y| e^{i\Phi_y})$ determines the order parameter. In the simplest form the total free energy can be written as the sum of four terms:

$$F = F_L + F_m + F_{ep} + F_{el} . \tag{1}$$

The first term is the Ginzburg–Landau free energy up to fourth order,

$$F_L = \alpha(|\eta_x|^2 + |\eta_y|^2) + ((\beta_1 + \beta_2)/2)(|\eta_x|^4 + |\eta_y|^4) + (\beta_1 + \beta_2 \cos(2\Phi))|\eta_x|^2|\eta_y|^2 , \tag{2}$$

here $\alpha = \alpha_0(T - T_0)$, β_1 and β_2 are the fourth-order stability parameters and $\Phi = \Phi_x - \Phi_y$. The second term, F_m, describes the coupling to the ordered magnetic moment, $\boldsymbol{m} = m(1, 0, 0)$, acting as a symmetry-breaking field:

$$F_m = -\gamma' m^2(|\eta_x|^2 + |\eta_y|^2) - \gamma m^2(|\eta_x|^2 - |\eta_y|^2) . \tag{3}$$

It consists of a symmetric term (proportional to γ') and a term that breaks the in-plane symmetry (proportional to γ). It is easy to show that, in the case of broken in-plane symmetry, minimization of the first two contributions to F (eq. (1)) and stability criteria lead to a splitting of the superconducting phase transition, where the upper transition at T_c^+ is to the (1, 0) phase ($\Phi = 0$) and the lower transition at T_c^- is to the (1, i) phase ($\Phi = \pm\pi/2$). These superconducting phases are labeled A and B in fig. 1, respectively. The ratio of the specific heat steps at the two transitions is given by $\Delta_{AB}c/\Delta_{NA}c = \beta_2/\beta_1$ (Δ defines the thermodynamic step). Under a magnetic field, gradient terms are added to F_L and F_m. The analysis of the upper critical fields at both transitions leads to a kink in B_{c2},

above which a third phase is found. This is the (0,1) phase, labeled C.

The third term, F_{ep}, describes in lowest order the coupling of the superconducting OP to the strains, ε_{kl},

$$F_{ep} = (g_v(\varepsilon_{xx} + \varepsilon_{yy}) + g'_v\varepsilon_{zz})(|\eta_x|^2 + |\eta_y|^2) + g_{66}(\varepsilon_{xx} - \varepsilon_{yy})(|\eta_x|^2 - |\eta_y|^2) + 2g_{66}\varepsilon_{xy}(\eta_x^*\eta_y + \eta_x\eta_y^*) . \quad (4)$$

It consists of a symmetric term that couples to the longitudinal strains (proportionality constants g_v and g'_v) and a symmetry-breaking term that couples to shear strains in the basal plane (g_{66}). The coupling of the strain to the superconducting OP leads in general to steps in the elastic constants c_{11}, c_{33} and c_{66} at the phase transitions, as observed in sound velocity measurements. The last term in eq. (1), F_{el}, is the elastic free energy.

It has already been pointed out by Thalmeier et al. [17] that only for the longitudinal elastic constants (c_{11} and c_{33}) have sizeable anomalies been observed at the phase transitions [5] and thus $g_{66} \ll g_v, g'_v$. Therefore, the symmetry-breaking term in eq. (4) is not significant. The important consequence of this result is that the splitting of T_c does not originate from lattice deformations via direct strain–superconducting OP coupling. The ratio of the steps in c_{11} and c_{33} at the phase transitions is given by: $\Delta_{AB}c_{11}/\Delta_{NA}c_{11} = \Delta_{AB}c_{33}/\Delta_{NA}c_{33} = \beta_2/\beta_1$. The measurements of the elastic constants [5] did not show steps in c_{11} or c_{33} at the AB transition, probably due to broadening of the transition.

A similar ratio can be derived [17] for the steps in α_c: $\Delta_{AB}\alpha_c/\Delta_{NA}\alpha_c = \beta_2/\beta_1$. The experimental thermodynamic steps $\Delta_{AB}\alpha_c$ and $\Delta_{NA}\alpha_c$ are of opposite sign and result in a negative ratio β_2/β_1 of -0.3 [12], in sharp contrast with the value of 0.4 [16] derived from the specific-heat data. For the steps in τ_c at the NC and NA phase lines, the model [17] predicts $1/R = \Delta_{NC}\tau_c/\Delta_{NA}\tau_c = \sqrt{(K_2/K_1)}$, where R represents the ratio of the upper critical field slopes $B'_{c2}(NC)/B'_{c2}(NA)$. The magnetostriction experiments [12] indicate a very small step at the NC transition compared to the step at the NA transition, resulting in $R \simeq 0$. This ratio differs largely from that deduced directly from B'_{c2}: $R \simeq 1.28$ (see fig. 2).

The discrepancies inferred from the dilatometry study yield serious problems for the GL analysis that cannot be solved by taking into account the direct strain–superconducting OP coupling. Therefore, we have investigated the effect of taking into account higher-order terms in eq. (4). This effect can be estimated from the slopes of the thermodynamic quantities at the phase transitions. It appears, however, to be far too small to explain, for instance, the experimental ratio of steps in α_c. Finally, we have investigated the influence of a coupling of the strains to the SBF [17]. Incorporating this effect appears to be crucial in order to explain the results. It should be strongly anisotropic, however, in order to explain the anisotropic pressure experiments.

4. Interplay of antiferromagnetism and superconductivity

In the most elaborate Ginzburg–Landau models it is assumed that the reduced-moment antiferromagnetism at $T_N = 5$ K provides the symmetry-breaking field. Recently, some evidence for this was put forward by neutron scattering [18] and specific heat [19] experiments under hydrostatic pressure, which showed that both the AF moment and the splitting $\Delta T_c = T_c^+ - T_c^-$ vanish at a critical pressure $p_c \simeq 4$ kbar. However, more convincing evidence was deducted from the observation that ΔT_c is proportional to the AF moment squared $m^2(T_c^+)$, independent of pressure, in accordance with theory [9]. The high-precision phase diagram, particularly the anomalous behaviour of the AB phase line near 0.1 T (fig. 2), might provide further support for a coupling of the magnetic and superconducting order parameters. The above-mentioned low-field anomaly in $\lambda_c(B)$ at 0.1 T (denoted by B_d) weakens at increasing the temperature, and is no longer observed at 4.4 K, suggesting that it is related to the AF order. The anomaly in λ_c (B) appears as a temperature-independent phase line at $B_d = 0.1$ T (see fig. 2). This phase line intersects the AB phase line just where the slope changes, which strongly suggests that both phenomena are coupled. As the low-field anomaly at B_d displays some hysteresis, we suggest that it arises from small lattice distortions caused by the reorientation of magnetic domains towards a direction perpendicular to the field. Assuming the two-dimensional E_{1g} representation for the order parameter, the slopes of the phase lines AN and AB have been investigated in the GL approach, for various orientations of the SBF with respect to the magnetic field [9]. Within this framework the kink in the AB phase line can be explained by a crossover from an averaging random in-plane (along the b-axes) orientation, yielding parallel phase lines NA and AB, to the configuration SBF $\perp B$ for $B > 0.1$ T, when all domains are oriented perpendicular to the field. However, further detailed magnetostriction studies for various orientations of the magnetic field (in the (a, b)-plane and along the hexagonal axis) are needed to verify this hypothesis. Also neutron scattering measurements in field will be extremely helpful.

5. The effect on T_c by alloying

In order to further investigate the superconducting phase diagram of UPt_3 we have started a series of alloying experiments. Recently, the effects of substituting Pt (5d element) by iso-electronic Pd (4d) [20,21], and U by Th [22] or Y [21] (non-f-electron elements) have been investigated. Electrical-resistivity and specific-heat studies have revealed that the superconducting state is extremely sensitive to impurities. Very low impurity concentrations (of the order of 1 at%) are already effective in suppressing superconductivity completely. In the course of a more systematic investigation, we here report on two other substitutions on the Pt lattice, namely, the 5d elements Ir and Au. Electrical-resistivity measurements were performed in order to determine T_c (or more precisely T_c^+) and the residual resistance, ρ_0, as function of impurity contents. The results obtained on annealed (7 days at 900°C) polycrystalline samples are shown in fig. 4. For comparison, we also show the results for Pd (fig. 4) and Th and Y doping (fig. 5). In order to compare the effects of substitution on the U and Pt lattice, we have plotted T_c^+ and ρ_0 as function of the absolute impurity contents x or y as defined by the composition $U_{1-x}A_xPt_{3-y}B_y$, where A denotes Th or Y and B denotes Pd, Ir or Au. Because the geometrical factors for the determination of ρ_0 could not always

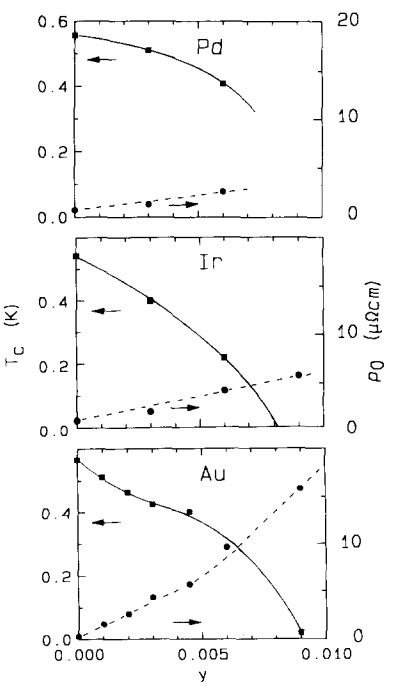

Fig. 4. T_c^+ (■) and ρ_0 (●) as function of impurity concentration y in $UPt_{3-y}B_y$, where B denotes Pd or Ir or Au. Solid and dashed lines are guides to the eye.

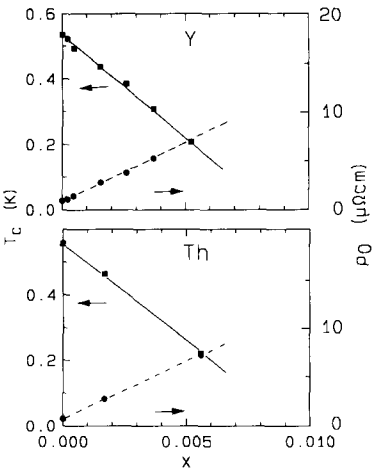

Fig. 5. T_c^+ (■) and ρ_0 (●) as a function of the impurity concentration x in $U_{1-x}A_xPt_3$, where A denotes Y or Th. Solid and dashed lines are guides to the eye.

be determined with high accuracy, the room-temperature resistivity values were normalized to 240 μΩ cm [1]. The data in figs. 4 and 5 show a smooth variation in T_c^+ for each substitution, although a clear correlation between the various substitutions is not easily detected. For Y and Th doping, the suppression of T_c^+ occurs in a similar, close to linear, way. In the case of Pd, Ir and Au doping, the suppression of T_c^+ is strongly nonlinear. The initial suppression is slowest for Pd. On the other hand, for these low impurity concentrations, ρ_0 increases almost linearly and at the same rate for Y, Th and Au doping, while ρ_0 increases much more slowly for Pd and Ir doping.

The resistivity measurements performed so far yield little systematics. No significant trends for doping on the U lattice on the one hand, and doping on the Pt lattice on the other, have been observed, although the latter type of substitution reveals a more anomalous behaviour. Specific-heat measurements on the Pd doped series showed a remarkable increase in the splitting of T_c (ΔT_c) with increasing Pd content, whereas for Y doping ΔT_c remained constant [21]. In the GL approach, the increase in ΔT_c points to a strengthening of the SBF. As in the $UPt_{3-y}Pd_y$ series ($0.03 < y < 0.30$) a large antiferromagnetically ordered moment stabilizes [20] (which is not the case for Y doping), we have suggested that the increase in ΔT_c is directly related to the increase in the size of the ordered moment, thus proving the origin of the SBF [21]. Long-range AF order is also induced by Th and Au doping (but not by Ir doping) [1] (and references therein) and we therefore expect to observe a similar increase in ΔT_c in these series. However, this is not confirmed by $c(T)$ data for the Th-doped samples [22], while $c(T)$ measurements on the Au-doped samples are under way. Also the data in figs. 4 and 5 do not

show clear-cut differences between doping with Pd, Au and Th (leading to magnetic order) on the one hand, and doping with Y and Ir (no magnetic order) on the other.

From the data in figs. 4 and 5 it is evident that small amounts of impurities have large effects on the unconventional superconducting state of UPt_3. Because the elements substituted so far are not magnetic, they are considered to create Kondo holes, which act strongly pair breaking. As a result, strong deviations from the ordinary Abrikosov–Gorkov pair breaking mechanism are expected. Finally, we note that doping with boron [23] leads to a considerable increase in T_c (=556 mK for a single-crystalline sample) and a decrease in ρ_0 (0.26 $\mu\Omega$ cm for $I \| c$). Although the increase in T_c can partly be explained by a negative chemical pressure (boron occupies interstitial sites), it is mainly attributed to a purification process during the sample preparation procedure (binding of oxygen by boron).

6. Concluding remarks

The recent experimental observations of additional anomalies in the thermodynamic properties of the superconducting phase of UPt_3 undoubtedly evidence unconventional superconductivity. The superconducting phase diagram can be explained to a large extent in a Ginzburg–Landau approach that includes a coupling of the superconducting order parameter to a symmetry-breaking field. However, as has been pointed out, several severe constraints on the stability parameters and the SBF have been noticed. It is therefore of interest also to explore other GL approaches, such as the scenario of two nearly degenerate representations that split the superconducting phase transition in the presence of a spontaneous lattice deformation or stacking faults [11]. The relevance of the latter scenario might be unveiled by a careful study of the crystalline perfection of the UPt_3 samples [24].

The work of one of us (AdV) was made possible by a fellowship of the Royal Netherlands Academy of Arts and Sciences. This work was part of the research program of the Dutch Foundation for Fundamental Research of Matter (FOM).

References

[1] A. de Visser, A. Menovsky and J.J.M. Franse, Physica B 147 (1987) 81.
[2] B.S. Shivaram, Y.H. Jeong, T.F. Rosenbaum, D.G. Hinks and S. Schmitt-Rink, Z. Phys. B 35 (1987) 5372.
[3] F. Gross-Alltag, B.S. Chandrasekhar, D. Einzel, P.J. Hirschfeld and K. Andres, Z. Phys. B 82 (1991) 243; C. Broholm, G. Aeppli, R.N. Kleiman, D.R Harshman, D.J. Bishop, E. Bucher, D.L. Williams, E.J. Ansalo and R.H. Heffner, Phys. Rev. Lett. 65 (1990) 2062.
[4] R.A. Fisher, S. Kim, B.F. Woodfield, N.E. Phillips, L. Taillefer, K. Hasselbach, J. Flouquet, A.L. Giorgi and J.L. Smith, Phys. Rev. Lett. 62 (1989) 1411.
[5] G. Bruls, D. Weber, B. Wolf, P. Thalmeier, B. Lüthi, A. de Visser and A. Menovsky, Phys. Rev. Lett. 65 (1990) 2294.
[6] S. Adenwalla, S.W. Lin, Q.Z. Ran, Z. Zhao, J.B. Ketterson, J.A. Sauls, L. Taillefer, D.G. Hinks, M. Levy and B.K. Sarma, Phys. Rev. Lett. 65 (1990) 2298.
[7] K. Hasselbach, A. Lacerda, K. Behnia, L. Taillefer, J. Flouquet and A. de Visser, J. Low Temp. Phys. 81 (1990) 299.
[8] K. Hasselbach, L. Taillefer and J. Flouquet, Phys. Rev. Lett. 63 (1989) 93.
[9] R. Joynt, Superc. Sci. Technol. 1 (1988) 210; K. Machida, M. Ozaki and T. Ohmi, J. Phys. Soc. Jpn. 58 (1989) 4116; D.W. Hess, T. Tokuyasu and J.A. Sauls, J. Phys.: Condens. Matter 1 (1989) 8135.
[10] G. Aeppli, E. Bucher, C. Broholm, J.K. Kjems, J. Baumann and J. Hufnagl, Phys. Rev. Lett. 60 (1988) 615.
[11] R. Joynt, J. Magn. Magn. Mater. 108 (1992) 31.
[12] N.H. van Dijk, A. de Visser, J.J.M. Franse, S. Holtmeier, L. Taillefer and J. Flouquet, to be published.
[13] S.K. Yip, T. Li and P. Kumar, Phys. Rev. B 43 (1991) 2742.
[14] A. Adenwalla, J.B. Ketterson, S.K. Yip, S.W. Lin, M. Levy and B.K. Sarma, to be published.
[15] D.S. Jin, S.A. Carter, B. Ellman, T.F. Rosenbaum and D.G. Hinks, Phys. Rev. Lett. 68 (1992) 1597.
[16] T. Vorenkamp, E.A. Knetsch, E. Wester, A. de Visser, A.A. Menovsky and J.J.M. Franse, to be published.
[17] P. Thalmeier, B. Wolf, D. Weber, G. Bruls, B. Lüthi and A.A. Menovsky, Physica C 175 (1991) 61.
[18] S.M. Hayden, L. Taillefer, C. Vettier and J. Flouquet, Phys. Rev. B 46 (1992) 8675.
[19] T. Trappmann, H. von Löhneysen and L. Taillefer, Phys. Rev. B 43 (1991) 13 714.
[20] A. de Visser, J.C.P. Klaasse, M. van Sprang, J.J.M. Franse, A. Menovsky, T.T.M. Plastra and A.J. Dirkmaat, Phys. Lett. A 113 (1986) 489.
[21] M.C. Aronson, T. Vorenkamp, Z. Koziol, A. de Visser, K. Bakker, J.J.M. Franse and J.L. Smith, J. Appl. Phys. 69 (1991) 5487.
[22] T. Vorenkamp, Z. Koziol, K. Bakker, J.J.M. Franse, M.C. Aronson and J.L. Smith, to be published.
[23] T. Vorenkamp, Z. Tarnawski, H.P. van der Meulen, K. Kadowaki, V.J.M. Meulenbroek, A.A. Menovsky and J.J.M. Franse, Physica B 163 (1990) 564.
[24] M.C. Aronson, R. Clarke, B.G. Demczyk, B.R. Coles, J.L. Smit, A. de Visser, T. Vorenkamp and J.J.M. Franse, Physica B 186–188 (1993) 788.